Comments and Addenda

The section Comments and Addenda is for short communications which are not appropriate for regular articles. It includes only the following types of communications: (1) Comments on papers previously published in **The Physical Review** *or* **Physical Review Letters**. *(2) Addenda to papers previously published in* **The Physical Review** *or* **Physical Review Letters**, *in which the additional information can be presented without the need for writing a complete article. Manuscripts intended for this section must be accompanied by a brief abstract for information-retrieval purposes. Accepted manuscripts follow the same publication schedule as articles in this journal, and page proofs are sent to authors.*

Measurement of $nd \rightarrow (n+1)p$ intervals in sodium Rydberg states*

W. E. Cooke, T. F. Gallagher, R. M. Hill, and S. A. Edelstein
Molecular Physics Center, SRI International, Menlo Park, California 94025
(Received 24 June 1977)

We report the measurement of $nd \rightarrow (n+1)p$ intervals in sodium Rydberg states with $n = 30$–32. The measurements were made using a microwave-resonance technique which utilizes selective field ionization. Fine-structure intervals of the p state are reported and shown to continue the $(n^*)^{-3}$ scaling law, where $n^* = n - \delta$ is the effective quantum number and δ is the quantum defect. Quantum defects for the p states are derived and compared to spectroscopic measurements.

Recently, techniques have been developed for measuring Δl intervals (i.e., *nd-nf*, *nd-ng*, and *nd-nh*) in alkali systems using microwave resonance techniques.[1] These techniques are inherently far more accurate for measuring small intervals than optical spectroscopy since the frequencies can be measured with very high precision using counting techniques, whereas spectroscopic techniques involve difficult comparisons of wavelengths. Using these measurements of the Δl intervals, Freeman and Kleppner[2] have demonstrated how to calculate the quantum defects of sodium states of $l \geq 2$ to accuracies as high as 2×10^{-6}. By measuring nd-$n+1$ p intervals, we have extended this precision to sodium p states.

In order to use our present microwave generators and measurement techniques, we were restricted to frequencies in the 30–40-GHz range, corresponding to nd-$n+1$ p transitions for $n \approx 30$. This makes optical detection, the method previously used to measure Δl transitions, virtually impossible since a $30p$ state in sodium has a radiative lifetime of nearly 0.2 ms. With such a long lifetime, the small amount of flourescence light would be very hard to detect above a photomultiplier dark current. Consequently, we have measured the nd-$n+1$ p transitions using selective-field ionization (SFI) to detect populations in the p state. The basic idea of this method is to populate the nd state initially, but to set the ionizing field so as to ionize only the $n+1$ p state. Thus, ordinarily, there is no field ionization. If we apply a microwave field and sweep its frequency through the nd-$n+1$ p resonance, we see a sharp increase in the ionization signal. This technique was first used for rf resonance detection by Gallagher *et al.* to measure sodium p- and d-state fine-structure intervals and polarizabilities,[3] although it has been extensively used by others as a Rydberg-state detector.[4]

In order to use SFI to perform resonance experiments, we must first understand the field ionization behavior of the states involved. Since this is treated extensively in Ref. 5, we shall only outline the main features. The threshold field required to ionize a state (with an ionization rate of 10^7 s^{-1}) is proportional to the square of the binding energy of the state in the high ionizing field. Under the conditions of our experiment, field slew rates of 10^8 V/cm s, the passage from the low field to the high ionizing field should be adiabatic, which implies that the energy ordering of the states in the high ionizing field is the same as it is in the low fields. Finally, the energy spacing of all the levels in high fields have been observed to be more or less uniform, especially for $m = 0$ states.[6] This approximate behavior is illustrated in Fig. 1. The classical ionization threshold, and its dependence on binding energy, is represented by the dashed line.

Using this model, we find that the $31d$ and $31p$ states, for example, are adiabatically connected to almost adjacent manifold states in the high field, which are separated by only ~ 0.2 cm^{-1}.

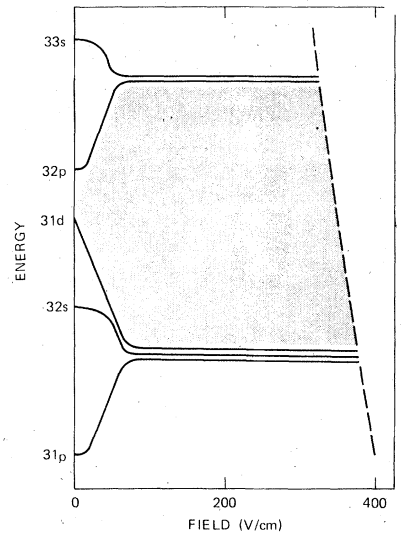

FIG. 1. Approximate location of $m=0$ states near the $n=31$ manifold. Within the shaded region are 28 states which are approximately equally spaced. Each state crosses the dashed boundary line at its classical ionization threshold.

Thus, although the states are well resolved in low field, by 6.5 cm^{-1}, their ionization thresholds differ by only 1%—clearly difficult to separate by SFI. On the other hand, the $31d$ and $32p$ states, while energetically close in zero field (1 cm^{-1}) are adiabatically connected to extreme upper and lower states of the $n=31$ manifold. In this case, the high-field energy separation is 8 cm^{-1}, leading to a difference in ionization thresholds of nearly 13%; consequently, it is quite easy to field ionize the $32p$ state without ionizing the $31d$ state.

In a sense, then, the $nd \rightarrow n+1\ p$ transition is an ideal case to study using SFI, for although the

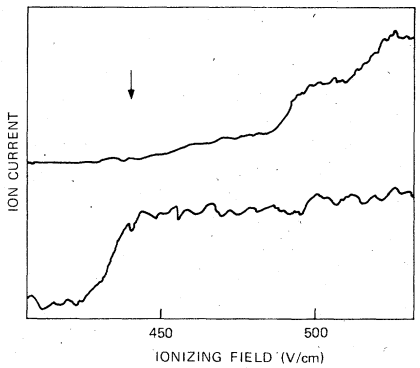

FIG. 2. Ionization thresholds for the $31d$ (upper curve) and $33s$ (lower curve) states. The arrow designates the field at which the ionizer was set to ionize the $32p$ state without ionizing the $31d$ state.

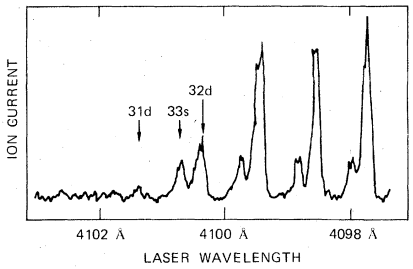

FIG. 3. Scan of the blue laser with the ionizer set at 445 V/cm to demonstrate the selective ionization of the $33s$ state. The similarity of the $33s$ and $32p$ ionization thresholds implies that the $32p$ state will also be ionized without ionizing the $31d$ state with this ionization field.

states lie relatively close to each other in low field, they correlate to the extremes of the Stark manifold and are easily distinguishable by field ionization. As shown in Fig. 1, $np \rightarrow n+1\ s$ is essentially the opposite case; states which are well resolved in zero field but correlate to adjacent manifold states in high field and are hence practically indistinguishable in field ionization.

Since the $n+1\ s$ and np states are expected to have more or less the same ionization thresholds (for $|m|=0$) we initially set the ionizing field using only s and d states. Thus to set the field for the $31d \rightarrow 32p$ measurements we investigated the ionization thresholds of the $31d$ and $33s$ states. Figure 2 shows the total ionization current of these two states versus the maximum height of the ionization pulse. As shown by Fig. 2, an ionization field of 445 V/cm should selectively ionize the $33s$ but not the $31d$ state. Accordingly the ionizing field was set to 445 V/cm, and we scanned the laser wavelength to sequentially populate the s and d Rydberg series, with the result shown in Fig. 3. Note the sudden increase in ionization efficiency occuring at the $33s$ state. As expected, the d states in general display stronger signals than the s states due to their higher multiplicity. However, the $32d$ state is an obvious exception. It is not completely ionized by the ionizing field of 445 V/cm because the $|m|=2$ component of the d state ionizes at a higher field, as is shown by the presence of "steps" in the ionization threshold.[7] SFI thus allows a resolution of ionization thresholds which is finer than the width of an individual threshold.

The actual experimental arrangement has been previously described in detail, so we shall only present an outline. A sodium beam passes between two parallel plates, where the sodium atoms are pumped stepwise by two tunable pulsed dye lasers through the $3p_{1/2}$ state into the $nd_{3/2}$ state (see Fig. 4). The Rydberg atoms are irradiated by microwaves which drive transitions to the

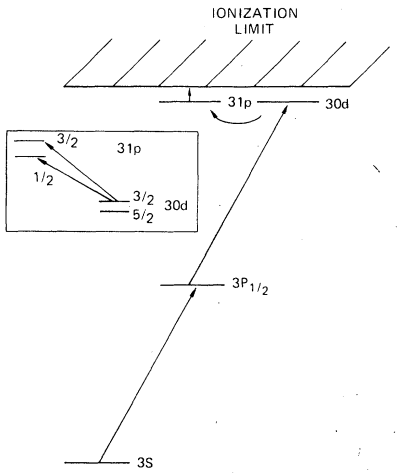

FIG. 4. Term diagram for Na showing the relevant states for measuring the $30d$-$31p$ transitions. The yellow laser populates the $3p_{1/2}$ state and the blue laser drives the $3p_{1/2}$-$30d_{3/2}$ transition. Microwaves cause transitions to either of the two $31p$ states which are then selectively ionized by field ionization.

$n+1\ p_{1/2}$ or $n+1\ p_{3/2}$ states. After 1 μs, the lower plate is pulsed to a high positive voltage (450 V for $n=31$) ionizing the $n+1\ p$ state atoms and forcing the ions through a grid in the top plate and into an electron multipler. The ion pulse is then sampled by a boxcar averager. Figure 5 shows two typical oscilloscope traces, each generated during a single laser pulse. The upper trace clearly shows ions from the $n+1\ p$ state when the microwave frequency was on resonance. The lower trace, generated with the microwaves off-resonance, shows that most of the noise in the trace is rf pickup generated by the firing of the laser. This noise formed a constant background which could be easily subtracted from the resonance

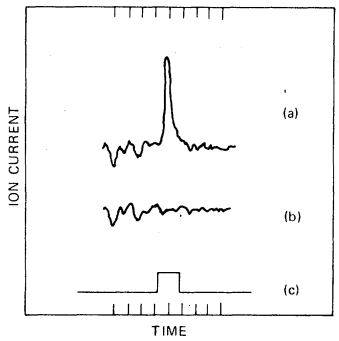

FIG. 5. Typical ionization signals obtained with a single shot of the lasers. Ionization signal (a) was generated with the microwaves on resonance; ionization signal (b) was generated with the microwaves off-resonance. The boxcar gate position is shown by (c). The time scale is 200 ns per division.

TABLE I. Transition frequencies (MHz) for $nd \rightarrow n+1\,p$ transitions in sodium.

n	$nd_{3/2} \rightarrow n+1\,p_{1/2}$	$nd_{3/2} \rightarrow n+1\,p_{3/2}$
30	38 572.0(40)	38 771.8(40)
31	34 967.9(50)	35 144.6(50)
32	31 801.4(40)	31 963.4(40)

signal. The gate of the boxcar averager was only open during the time when the strong resonance signal appears, as shown in Fig. 5.

The microwaves are generated by doubling the 15–21-GHz output of an HP628A klystron oscillator with a microwave diode. The microwave power was delivered to the interaction region via r band waveguide and an r band microwave horn. (This also served the purpose of filtering out the fundamental frequency.) The microwave frequency was measured by directing 1% of the fundamental microwave power through a wavemeter which was set twice during each frequency sweep: once near the $nd_{3/2} \rightarrow n+1\ p_{3/2}$ transition and once near the $nd_{3/2} \rightarrow n+1\ p_{3/2}$ transition. As the frequency was swept, one pen of a dual pen recorder monitored the ion signal from the boxcar integrator and one pen monitored the power transmitted through the wavemeter. Both increasing and decreasing frequency sweeps were taken to cancel the offset produced by the boxcar averager. The wavemeters were calibrated using an HP5340A microwave counter. We estimate the accuracy of this frequency measurement procedure to be ± 1 MHz.

Table I lists the frequencies of the six observed transitions. The numbers in parentheses represent one standard deviation confidence in the last digit of the reported number. The linewidths of the transitions were typically 6–10 MHz with some evidence of asymmetry. Figure 6 shows a typical

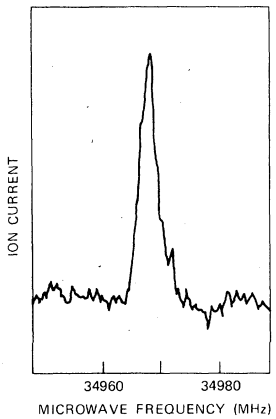

FIG. 6. Typical $31d_{3/2}$-$32p_{1/2}$ resonance taken with the microwave frequency increasing.

TABLE II. Fine-structure intervals of 31–33 p states in sodium.

n	S_p (MHz)	$(n^*)^3 S_p$ (cm^{-1})
31	199.3(20)	182(2)
32	177.0(30)	178(3)
33	162.2(25)	180(3)

$31d_{3/2}$-$32p_{1/2}$ resonance taken with the frequency increasing. This large linewidth and the asymmetry is mostly due to the Stark effect generated by the small residual electric fields. The presence of the earth's magnetic field only accounts for linewidths of 2–3 MHz. Calculations[3] show that the polarizability of the 30d state should be of the order 300 MHz/(V/cm)^2 so that even a very small (~0.1 V/cm) electric field could cause noticeable broadening. The −2.3-kV potential applied to the face of the electron multiplier generated a field of nearly 0.8 V/cm in the interaction region, even though the electron multiplier was 3 cm above the grid in the top plate and there was an additional grounded grid between the top plate and the electron multiplier. We were able to almost, but not quite, cancel this field by applying a positive potential to the top plate. From the line asymmetries, we have estimated the remaining shifts due to residual fields; these estimations are the primary limitation of the accuracy of the measurements.

The fine-structure (fs) intervals of the $n+1$ p states are the differences of the two frequencies for each nd-$n+1$ p transition. The fine-structure intervals for the 31–33 p states are listed in Table II. Since electric fields change the fs intervals only by the tensor polarizability of the p states, the fs intervals are less sensitive to stray fields than are the d-p intervals, by a factor of 50. Thus, the primary limitation of the accuracy of the p-state fine structures is the frequency-measurement system. In Fig. 7, we have plotted $(n^*)^3$ times the p-state fine-structure interval to show that the $(n^*)^{-3}$ scaling is continued to $n=33$. A systematic study of the d-state fine structures was not attempted since the d-state fs intervals are so small (<4 MHz) that the earth's magnetic field creates a significant perturbation. Furthermore, such measurements would be more susceptible to stray electric fields than are the p-state fs intervals because of the larger polarizability of the d states.

TABLE III. Quantum defects and binding energies of 31–33 p states.

n	W (cm^{-1})	δ_p	δ_p [a]
31	120.757 3(2)	0.855 00(4)	0.855 013
32	113.127 3(2)	0.855 00(4)	0.855 005
33	106.198 1(2)	0.854 98(4)	0.854 998

[a] Calculated by Risberg's extrapolation formula (Ref. 9).

The $nd \rightarrow n+1$ p transition frequencies may be adjusted for the d and p fine-structure intervals to yield the separation of the centers of gravity of the d and p states. The binding energy and quantum defects of the nd state may be calculated by the algorithm developed by Freeman and Kleppner,[2] thereby allowing the determination of the $n+1$ p-state binding energy and quantum defect. Table III lists these quantities for the 31–33 p states. In Fig. 8, we have plotted these quantum defects in addition to the $n=10$–32 p-

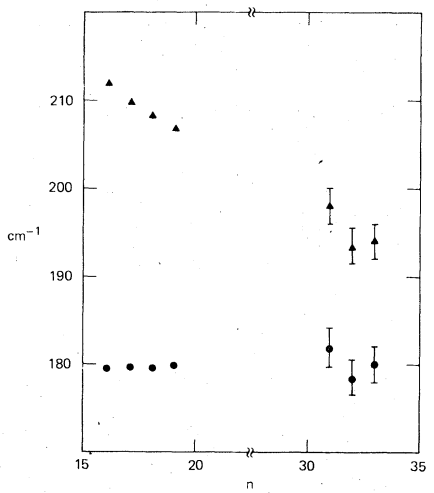

FIG. 7. Plot of $(n^*)^3 S_p$ (●) and $n^3 S_p$ (▲) vs n demonstrating the $(n^*)^3$ scaling. The data for states 16–19 are from Ref. 3.

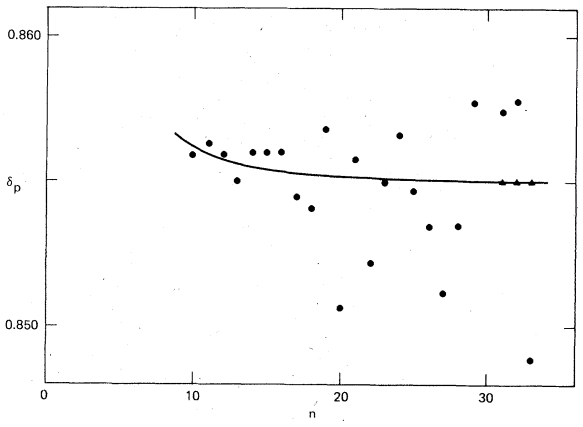

FIG. 8. Comparison of the p-state quantum defects obtained here (▲) with those (●) obtained spectroscopically by Thackeray (Ref. 8). The solid line is the extrapolation formula of Risberg (Ref. 9).

state quantum defects obtained by Thackeray from the absorption spectrum of Na.[8] The scatter in spectroscopic quantum defects represents a scatter of only 0.003 Å in the wavelength measurements. The solid line is the extrapolation formula which Risberg constructed by fitting the energies of the $n = 3$-7, np states to an extended Ritz formula.[9] The agreement with our values is well within our experimental uncertainty as shown in Table III, and thus confirms the limiting behavior of the formulas.

Note added in proof. It has been brought to our attention that recent measurements of C. Fabre, S. Haroche, and P. Goy [Phys. Rev. A (to be published)], which used SFI to detect microwave transitions in the 300-GHz regime, have determined the fine structure and quantum defects of the 31p and 32p states of sodium. These measurements agree with ours within their reported uncertainty of ± 30 MHz.

ACKNOWLEDGMENTS

We would like to acknowledge the generous loans of microwave equipment by S. Tetenbaum and G. Tomlin.

*Work supported by the Air Force Office of Scientific Research.

[1]T. F. Gallagher, R. M. Hill, and S. A. Edelstein, Phys. Rev. A 13, 1448 (1976); 14, 744 (1976).

[2]R. R. Freeman and D. Kleppner, Phys. Rev. A 14, 1614 (1976).

[3]T. F. Gallagher, L. M. Humphrey, R. M. Hill, W. E. Cooke, and S. A. Edelstein, Phys. Rev. A 15, 1937 (1977).

[4]See, for example, T. W. Ducas, M. G. Littman, R. R. Freeman, and D. Kleppner, Phys. Rev. Lett. 35, 366 (1975); R. F. Stebbings, C. J. Latimer, W. P. West, F. B. Dunning, and T. B. Cook, Phys. Rev. A 12, 1453 (1975); J. E. Bayfield and P. M. Koch, Phys. Rev. Lett. 33, 258 (1974); and C. Fabre, P. Goy, and S. Haroche, J. Phys. B 10, L183 (1977).

[5]T. F. Gallagher, L. M. Humphrey, W. E. Cooke, R. M. Hill, and S. A. Edelstein, Phys. Rev. A 16, 1098 (1977).

[6]M. G. Littman, M. L. Zimmerman, T. W. Ducas, R. R. Freeman, and D. Kleppner, Phys. Rev. Lett. 36, 788 (1976).

[7]T. F. Gallagher, L. M. Humphrey, R. M. Hill, and S. A. Edelstein, Phys. Rev. Lett. 37, 1465 (1976).

[8]E. R. Thackeray, Phys. Rev. 75, 1840 (1949); also reported in C. E. Moore, Atomic Energy Levels, Vol. 1, Natl. Bur. Stds. (U.S.) Circ. No. 467 (U.S. GPO, Washington, D.C., 1949), p. 89.

[9]P. Risberg, Ark. Fys. 10, 583 (1956).